New Phytologist

Research

Daytime stomatal regulation in mature temperate trees prioritizes stem rehydration at night

Richard L. Peters[1,2,3], Kathy Steppe[1], Christoforos Pappas[4], Roman Zweifel[2], Flurin Babst[5,6], Lars Dietrich[7], Georg von Arx[2,8], Rafael Poyatos[9,10], Marina Fonti[2], Patrick Fonti[2], Charlotte Grossiord[11,12], Mana Gharun[13,14], Nina Buchmann[13], David N. Steger[7] and Ansgar Kahmen[7]

[1]Laboratory of Plant Ecology, Department of Plants and Crops, Faculty of Bioscience Engineering, Ghent University, Coupure links 653, B-9000 Ghent, Belgium; [2]Forest Dynamics, Swiss Federal Research Institute for Forest, Snow and Landscape Research (WSL), Zürcherstrasse 111, CH-8903 Birmensdorf, Switzerland; [3]Forest is Life, TERRA Teaching and Research Centre, Gembloux Agro Bio-Tech, University of Liège, Passage des Déportés 2, 5030 Gembloux, Belgium; [4]Department of Civil Engineering, University of Patras, Rio, Patras 26504, Greece; [5]School of Natural Resources and the Environment, University of Arizona, East Lowell Street 1064, Tucson, AZ 85721, USA; [6]Laboratory of Tree-Ring Research, University of Arizona, East Lowell Street 1215, Tucson, AZ 857121, USA; [7]Department of Environmental Sciences – Botany, University of Basel, Schönbeinstrasse 6, CH-4056 Basel, Switzerland; [8]Oeschger Centre for Climate Change Research, University of Bern, 3012 Bern, Switzerland; [9]CREAF, E08193 Bellaterra (Cerdanyola del Vallès), Catalonia, Spain; [10]Universitat Autònoma de Barcelona, E08193 Bellaterra (Cerdanyola del Vallès), Catalonia, Spain; [11]Plant Ecology Research Laboratory PERL, School for Architecture, Civil and Environmental Engineering, EPFL, CH-1015 Lausanna, Switzerland; [12]Community Ecology Unit, Swiss Federal Institute for Forest, Snow and Landscape WSL, CH-1015 Lausanne, Switzerland; [13]Department of Environmental Systems Science, ETH Zurich, Universitatstrasse 2, CH-8092 Zurich, Switzerland; [14]Department of Geosciences, University of Münster, Heisenbergstrasse 2, 48149 Münster, Germany

Author for correspondence:
Richard L. Peters
Email: richard.peters@unibas.ch

Received: *23 December 2022*
Accepted: *16 April 2023*

New Phytologist (2023) **239:** 533–546
doi: 10.1111/nph.18964

Key words: canopy conductance, dendrometer, European forests, hydraulic traits, leaf water potential, sap flow, stomatal control, wood anatomy.

Summary

- Trees remain sufficiently hydrated during drought by closing stomata and reducing canopy conductance (G_c) in response to variations in atmospheric water demand and soil water availability. Thresholds that control the reduction of G_c are proposed to optimize hydraulic safety against carbon assimilation efficiency. However, the link between G_c and the ability of stem tissues to rehydrate at night remains unclear.
- We investigated whether species-specific G_c responses aim to prevent branch embolisms, or enable night-time stem rehydration, which is critical for turgor-dependent growth. For this, we used a unique combination of concurrent dendrometer, sap flow and leaf water potential measurements and collected branch-vulnerability curves of six common European tree species.
- Species-specific G_c reduction was weakly related to the water potentials at which 50% of branch xylem conductivity is lost (P_{50}). Instead, we found a stronger relationship with stem rehydration. Species with a stronger G_c control were less effective at refilling stem-water storage as the soil dries, which appeared related to their xylem architecture.
- Our findings highlight the importance of stem rehydration for water-use regulation in mature trees, which likely relates to the maintenance of adequate stem turgor. We thus conclude that stem rehydration must complement the widely accepted safety–efficiency stomatal control paradigm.

Introduction

The emergence of stomata *c.* 400 million years ago was transformative for plants, because they gained a dedicated apparatus to balance the fixation of atmospheric CO_2 against the loss of H_2O across terrestrial ecosystems (Edwards *et al.*, 1998; Buckley, 2019). This critical function of stomata has been known for over a century (Darwin, 1898), and its relevance for the terrestrial carbon and water cycle is fundamental (Schlesinger & Jasechko, 2014; Mastrotheodoros *et al.*, 2020). Yet, recent observations and climate projections reveal prolonged periods of high vapour pressure deficit (D) and low soil water availability (i.e. low soil water potential; Ψ_{soil}) negatively affecting forest ecosystems (e.g. Novick *et al.*, 2016; Babst *et al.*, 2019; Wenping *et al.*, 2019; Buras *et al.*, 2020; Grossiord *et al.*, 2020; Hammond *et al.*, 2022). This insight has stimulated research that focusses on the mechanisms of stomatal conductance (g_s) regulation in mature trees during periods of low water availability (e.g. Fatichi *et al.*, 2016; Novick *et al.*, 2016).

The regulation of g_s, and ultimately the conductance of the entire tree canopy (G_c), is influenced by environmental factors (e.g. light, D and Ψ_{soil}), leaf CO_2 concentration, leaf water potential (Ψ_{leaf}), plant nutrients and plant hormones (Jarvis *et al.*, 1976; Schulze *et al.*, 1994; Damour *et al.*, 2010; Wang *et al.*, 2020). Modelling of g_s behaviour has been effective in reproducing the general pattern of reducing g_s in response to decreasing water availability based on the hydraulic safety-assimilation efficiency paradigm (Katul *et al.*, 2010; Sperry *et al.*, 2017; Anderegg *et al.*, 2018; Henry *et al.*, 2019). This paradigm could subsequently explain why the g_s response to decreasing soil water availability, increasing D and decreasing midday Ψ_{leaf}, varies substantially among tree species (as visualized in Fig. 1a; Comstock & Mencuccini, 1998; Oren *et al.*, 1999; Anderegg *et al.*, 2017; Grossiord *et al.*, 2017; Novick *et al.*, 2019; Gharun *et al.*, 2020; Flo *et al.*, 2021).

The species-specific differences in stomatal behaviour in response to decreasing Ψ_{leaf} (see λG_{c50} in Fig. 1a) have been used to characterize different water-use strategies of trees (Martínez-Vilalta & Garcia-Forner, 2017; but see Hochberg *et al.*, 2018 and Martinez-Vilalta *et al.*, 2019). Species-specific differences in G_c responses have been explained by differences in branch xylem vulnerability thresholds for embolism formation. In this context, the branch xylem water potential (Ψ_{xylem}) at which 50% or 88% of hydraulic conductivity is lost has been considered as a xylem vulnerability threshold (but see McCulloh *et al.*, 2014; McCulloh *et al.*, 2019). This measure has been described to effectively explain species-specific mortality risk (i.e. hydraulic failure; Anderegg *et al.*, 2016; Choat *et al.*, 2018; Arend *et al.*, 2021). A recent study by Joshi *et al.* (2022) combined stomatal control and xylem vulnerability into a model where they incorporated the cost of transpiration by including the risk of hydraulic failure, using stomatal optimization modelling (see also Wolf *et al.*, 2016). The results showed that the control of g_s is primarily meant to avoid the risk of embolism formation. They confirm the aforementioned safety–efficiency paradigm, where their simulations were validated with measurements obtained from herbs and juvenile trees grown in controlled drought experiments (fig. 5d in Joshi *et al.*, 2022). Based on this research, one could hypothesize that mature trees will show a stronger G_c control due to a lower xylem embolism resistance in the branches (Fig. 1b, hypothesis 1 = H1). However, evidence has been found that both supports (Brodribb & Holbrook, 2004; Anderegg *et al.*, 2017; Martin-StPaul *et al.*, 2017; Flo *et al.*, 2021) and falsifies (Bartlett *et al.*, 2016) this hypothesis. Thus, the overarching question remains whether species-specific differences in G_c response are driven by the goal of preventing hydraulic failure in the canopy of mature trees.

Alternatively, stomatal closure due to decreasing water availability could act towards sustaining turgor pressure within stem cambial tissues, allowing for growth. The gradual drop in tissue Ψ during periods of high D and low Ψ_{soil} severely impairs stem growth before any hydraulic damage occurs (Delzon & Cochard, 2014; Fatichi *et al.*, 2016; Walthert *et al.*, 2021). Lack of turgor pressure in the cambium has been identified as a critical limitation to xylem cell division and elongation in the stem (Steppe *et al.*, 2015; Fatichi *et al.*, 2019; Coussement *et al.*, 2021; Peters *et al.*, 2021b), and recent evidence supports its importance as a growth-limiting factor across biomes (Cabon *et al.*, 2022).

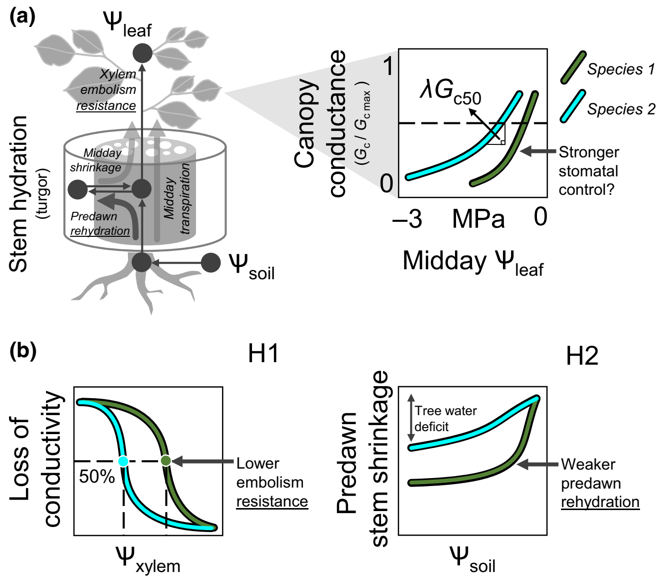

Fig. 1 Graphical representation of two hypotheses explaining species-specific stomatal control during lowered water availability. (a) Two contrasting mature tree species (species 1 dark green and species 2 in cyan) within the soil-tree-atmosphere continuum are presented, where water moves from the roots through the stem to the leaves during midday. At the same time, water is used from the stem tissue (i.e. bark) causing stem shrinkage, which is primarily replenished during the night to allow for turgor-dependent growth. Decreasing standardized canopy conductance (G_c/G_{cmax}) in response to decreasing midday leaf water potential (Ψ_{leaf}) reduces this loss of water from the tree, where we use the slope of this response at 50% of maximum conductance (λG_{c50}) to quantify species-specific reduction in canopy conductance. (b) Two contrasting hypotheses could explain the species-specific difference in λG_{c50} presented in (a). Hypothesis (H1): species 2 shows a lower λG_{c50} as it has a more negative branch xylem water potential (Ψ_{xylem}) at which 50% loss of conductivity is reached compared with species 1 – that is, lower embolism resistance in species 1 requires earlier stomatal closure during periods of lower water availability to safeguard from hydraulic damage. Hypothesis (H2): species 1 requires a higher λG_{c50} as predawn rehydration is more difficult to maintain during drought (i.e. lower soil water potential; Ψ_{soil}) for this species than for species 2, with increasing tree water deficit substantially affecting turgor-dependent growth – that is, λG_{c50} is higher because of sustained stem shrinkage at night during periods of lower Ψ_{soil} due to lower root–soil connectivity and/or lower hydraulic transport efficiency. H1 assumes that stomatal control during drought is solely steered towards retaining hydraulic safety in the canopy, whereas H2 assumes priority of stomatal control for maintaining hydration in the phloem and cambial zone of the stem, which is critical for radial stem growth.

Moreover, water loss from the phloem can cause turgor loss in the cambium, reducing the efficiency at which sugars are transported down from the canopy (De Schepper & Steppe, 2010; Lemoine *et al.*, 2013; Salmon *et al.*, 2019; Hubau *et al.*, 2020). The loss of stem water due to transpiration during the day causes the stem to shrink in size, as the root-water supply is slower than the water loss via transpiration (Steppe *et al.*, 2006), where the tree has to rehydrate to reduce this deficit (i.e. tree water deficit; Zweifel *et al.*, 2016) and restore turgor pressure within the stem's cambium tissue at night (Steppe *et al.*, 2015; Zweifel *et al.*, 2021; Etzold *et al.*, 2022). However, depending on both the species-specific root-water supply and the sapwood anatomical

Table 1 Characteristics of trees instrumented for continuous monitoring.

Species	Plant functional type	Tree code	d_{stem} (cm)	h_{tree} (m)	h_{stem} (m)	t_{sw} (cm)	t_{ba} (cm)	t_{phl} (mm)
Fagus sylvatica	Diffuse-porous	FASY1*	72.9	42.3	19.0	12.6	0.6	4
	Deciduous	FASY2*	59.6	33.0	18.1	9.9	0.8	4
	Broad-leaved	FASY3	57.0	35.0	18.0	9.9	0.6	4
		FASY4*	63.0	38.0	20.0	12.7	0.7	4
Carpinus betulus	Diffuse-porous	CABE1*	36.3	21.3	10.2	8.8	0.6	3
	Deciduous	CABE2*	32.5	23.8	7.9	10.5	0.5	4
	Broad-leaved	CABE3*	46.9	35.0	12.2	11.4	0.6	2.5
		CABE4*	34.6	24.6	14.5	10	0.4	3
Quercus petraea	Ring-porous	QUPE1*	52.9	35.8	13.4	1.5	1.4	5.0
	Deciduous	QUPE2*	48.5	21.9	13.6	1.0	2.0	4.0
	Broad-leaved	QUPE3*	50.0	21.0	14.7	2.6	1.3	5.0
		QUPE4*	47.3	22.0	13.8	2.5	2.2	6.0
Picea abies	Tracheid	PCAB1*	61.8	39.0	16.2	6.0	1.4	5.0
	Evergreen	PCAB2*	67.2	36.1	20.2	5.8	1.1	5.0
	Conifer	PCAB3*	57.8	40.2	18.5	5.3	1.5	4.0
		PCAB4*	60.2	37.5	19.0	5.2	1.8	5.0
Pinus sylvestris	Tracheid	PISY1	62.0	25.4	19.7	4.2	1.8	1.0
	Evergreen	PISY2*	45.0	41.0	28.7	8.5	1.8	2.0
	Conifer	PISY3*	51.4	40.0	29.6	8.5	2.2	1.5
		PISY4*	52.5	36.0	31.0	5.8	2.4	2.0
Larix decidua	Tracheid	LADE1	49.8	37.8	26.0	5	1.8	4
	Deciduous	LADE2	54.1	27.5	20.5	2.4	2.4	5
	Conifer	LADE3	48.4	38.4	24.8	2.2	2	4
		LADE4	56.4	39.2	25.6	1.9	2.2	4

For each tree, diameter at breast height (d_{stem}), tree height (h_{tree}), stem length (h_{stem}), sapwood thickness (t_{sw}), maximum bark thickness (t_{ba}) and phloem thickness (t_{phl}) were measured. The * symbol indicates the tree close to which we monitored soil water potential (Ψ_{soil}).

architecture (Peters *et al*., 2021b), increased predawn tree water deficit (TWD_{pd}) during drought can cause sustained low turgor pressure during the night (Zweifel *et al*., 2016; Salomón *et al*., 2022) and force stricter stomatal regulation to avoid further dehydration and turgor loss (Potkay & Feng, 2022). Although responses of TWD_{pd} to drought can be utilized to test whether species exhibit weaker predawn rehydration, we lack evidence, showing that mature trees indeed reduce G_c to prioritize predawn stem rehydration (Fig. 1b, H2). As such, it remains unclear whether the species-specific G_c control is tuned to sustain turgor (for growth) or avoid branch embolism formation while maximizing carbon assimilation at the cost of turgor loss in the phloem and cambial zone (McDowell *et al*., 2008; Kannenberg *et al*., 2019; Mantova *et al*., 2021; Potkay & Feng, 2022).

In this study, we assess the coupling between Ψ_{leaf} induced reduction in G_c in mature temperate tree species, with branch xylem embolism resistance and the potential for predawn stem rehydration (quantified by the response of predawn stem shrinkage to drought; Fig. 1). Specifically, we tested whether species-specific responses of G_c are better explained by branch xylem embolism vulnerability (Fig. 1b, H1) or predawn stem rehydration potential (Fig. 1b, H2). We also assessed whether lower predawn rehydration during drought is dependent upon the hydraulic resistance of the sapwood xylem, which hampers water transport back into the bark. Testing these hypotheses requires continuous canopy and tree stem measurements, as well as wood and branch sampling of individual mature trees, covering a wide range of wet and dry environmental conditions. The unique tree physiological measurements collected in a well-studied temperate forest in Switzerland (see Dietrich *et al*., 2019) allowed us to perform this study. Six common temperate tree species ranging from anisohydric *Quercus petraea* to isohydric *Pinus sylvestris* (i.e. Martínez-Vilalta & Garcia-Forner, 2017; Martínez-Sancho *et al*., 2017a) were monitored. We combined (bi-)weekly predawn and midday Ψ_{leaf} measurements collected for mature trees using a canopy crane, high-resolution sap flow measurements, percent conductance loss (PLC) curves from branches, automated dendrometer monitoring and quantitative wood anatomy (to contextualize stem shrinkage patterns with the hydraulic architecture).

Materials and Methods

Site description

The study site is located in a temperate forest near Hofstetten, Switzerland (47.469°N, 7.502°E). The dry period occurred in the summer of 2015, with only 96.6 mm of precipitation during July and August, placing it within the 10% driest summers over the past 100 yr at the study site (Dietrich & Kahmen, 2019). This resulted in soil water potential (Ψ_{soil}; see Supporting Information Table S1 for abbreviation overview) decreasing to −1.3 MPa and vapour pressure deficit (D) reaching up to 4 kPa from the beginning of July to mid-September (see Dietrich *et al*., 2019). Continuous monitoring was performed on six common European species with four mature individuals per species ($n = 24$ trees, Table 1), covering *Fagus sylvatica* L., *Carpinus betulus* L., *Q. petraea* (Matuschka) Liebl., *Picea abies* (L.) Karst, *P. sylvestris* L. and *Larix decidua* Mill.

General approach for hypotheses testing

To test the two hypotheses presented in Fig. 1, we quantified stomatal control using sap flow measurements and determined the steepness of the relative whole-tree canopy conductance slope (G_c/G_{cmax}; according to Peters *et al.*, 2019) to measured values of midday Ψ_{leaf} (e.g. Anderegg *et al.*, 2017). The slope (λ) between relative G_c and Ψ_{leaf} at 50% conductance (λG_{c50}) was used to characterize species-specific regulation of stomatal conductance in response to declining water availability. To test H1, we compared species-specific values of λG_{c50} against thresholds obtained from measured percentage loss of conductance (PLC) curves from branches. H2 was assessed by relating λG_{c50} to the predawn stem shrinkage patterns of a species obtained from point dendrometer data (Salomón *et al.*, 2022) and by relating species-specific predawn stem rehydration potential to wood anatomical features defining hydraulic resistance.

Continuous high-resolution measurements

All 24 trees were equipped with thermal dissipation sap flow sensors (SFS2-M; UP GmbH, Ibbenbüren, Germany; Granier, 1985) installed at 1.5 m height on the north-east side of the main tree bole according to the manufacturer's specifications. Two 20-mm-long probes were radially inserted into the xylem (underneath the cambium) with a vertical distance of 10 cm and shielded from direct sunlight. The temperature difference between the heated and unheated probe (ΔT in °C) was recorded every 10 min with a sensor node from April 2014 to October 2015 (Chanel Node, Decentlab GmbH, Switzerland).

On the same trees and during the same period, stem diameter variations (Δd_{stem} in μm) were recorded using automated point dendrometers (ZN11-T-WP; Natkon, Oetwil am See, Switzerland). These dendrometers were installed onto the outer bark of the stem at *c.* 2 m above ground on the north-facing side and recorded Δd_{stem} every 10 min. The outermost dead layer of bark under the dendrometer was carefully removed to minimize the effect of hygroscopic swelling, while avoiding damage to the living bark underneath. To reduce variance due to circumferential variability (i.e. Lu *et al.*, 2004), both dendrometer and sap flow measurements were collected on the same side of a stem (horizontal distance < 20 cm).

Air temperature (T_a in °C), relative humidity (%), solar irradiance (W m^{-2}), and precipitation (mm) were monitored using a weather station (Davis Vantage Pro 2; Scientific Sales Inc., Lawrenceville, NJ, USA) at 10-min intervals. Relative humidity and T_a were used to calculate D (kPa). Additionally, Ψ_{soil} (MPa) was measured (MPS-2; Decagon Devices, Pullman, WA, USA) at a soil depth of 20 cm, *c.* 2 m near the stems of 12 trees distributed across the site (see Table 1). Sensor failure did not allow us to use data collected at the remaining six trees. To represent the Ψ_{soil} dynamics at the site, we averaged the values measured from all sensors. All monitoring data were inspected for outliers using the DATACLEANR package (Hurley *et al.*, 2022) in the R software environment (v.4.0.2; R Core Team, 2017).

Branch and wood sampling

Tree water status was assessed on all trees by measuring midday (≈13:00 Central European Time; CET) and predawn (≈5:00 CET) Ψ_{leaf}. Branch sampling was performed to measure predawn and midday Ψ_{leaf} using a canopy crane *c.* every 7 d during the growing seasons of 2014 and 2015, with predawn measurements mainly performed in 2015. At each measurement date, three *c.* 10-cm-long terminal shoots were collected per tree with three to four leaves (for broad-leaved species) or current-year shoots (for conifer species) from the upper part of the sunlit canopy. Directly after sampling, Ψ_{leaf} was measured using a Scholander pressure bomb (Model 1000; PMS Instruments, Albany, OR, USA). Additionally, branches of *c.* 35 cm in length were collected for all species in October 2015 to establish PLC curves. These larger branches were collected from 24 trees (one additional tree, to the monitored four trees, for *F. sylvatica*, *P. abies* and *L. decidua*), almost fully overlapping with the monitored trees, as some *P. sylvestris* (PISY4) and *Q. petraea* (QUPE3 and QUPE4) trees were not safely accessible from the crane. After collection, the branch segments were wrapped into moist paper towels and stored at 4°C. For *Q. petraea*, we collected branch segments of *c.* 1.2 m in length due to the longer vessel length (see Dietrich *et al.*, 2019 for details).

Xylem flow resistance of the conducting sapwood tissue of the monitored trees was analysed using quantitative wood anatomy to contextualize predawn rehydration potential (see details below). To ensure sampling of the entire sapwood depth and enhance comparability with the ΔT and Δd_{stem} measurements, one wood core of *c.* 12 cm length was taken from each tree within 10 cm distance from the dendrometer in January 2019 (using an increment borer; Haglöf, Långsele, Sweden). In addition, we recorded multiple tree characteristics (Table 1), including diameter at breast height (d_{stem}), tree height (h_{tree}) and stem length (h_{stem}; using a Vertex IV; Haglöf), sapwood thickness (t_{sw}; visually determined from the collected tree cores, by detecting changes in translucence or colour), maximum bark (t_{ba}; measured at the four cardinal directions, including phloem and cork) and phloem thickness (t_{phl}).

Data processing to target physiological parameters

The ΔT measurements obtained from sap flow sensors were converted to sap flux density (F_d; kg m^{-2} s^{-1}) using the TREX R package (Peters *et al.*, 2021a) while applying (1) the double-regression method to establish zero-flow conditions (using a 5-d period), (2) sapwood corrections (using t_{sw}) and (3) species- (*F. sylvatica*, *P. abies* and *L. decidua*) or wood-specific (*P. sylvestris* = Coniferous, *Q. petraea* = Ring-porous and *C. betulus* = Diffuse-porous) calibrations (as calibration studies were not present for all species). G_c (in mol m^{-2} s^{-1}) was calculated according to Flo *et al.* (2021; Eqn 1).

$$G_c = \frac{(115.8 + 0.4236\ T_a)\ F_d}{D} \cdot \theta \cdot \frac{T_0}{(T_0 + T_a)} \cdot e^{-0.00012 \cdot h} \qquad \text{Eqn 1}$$

For each tree, we used the mean midday data (between 10:00 and 15:00 CET) to calculate G_c to reduce the impact of stem capacitance and delayed flow dynamics (see Pappas *et al.*, 2018; Peters *et al.*, 2019). Midday F_d, D and T_a were used, in combination with θ, which is equal to 44.6 mol m^{-3}, T_0, which is 273 K, and h (m), which is the elevation of the site. Daily mean G_c values were removed if $D < 0.3$ kPa and mean daily precipitation > 1 mm (see Peters *et al.*, 2019). As no information was available on the total leaf area and allometric equations seemed inadequate to reconstruct the total leaf area for all species (by using Forrester *et al.*, 2017), we standardized G_c and expressed it per unit of sapwood area to the maximum G_c per tree (G_{cmax} as the 99th percentile of G_c; following Anderegg *et al.*, 2016). Moreover, we excluded cloudy days (global irradiance < 150 W m^{-2} d^{-1}) and cold days ($T_a < 14$°C d^{-1}) to isolate optimal transpiration conditions (see Peters *et al.*, 2019).

Percentage loss of conductance curves were established by performing centrifuge measurements using the Cavitron technique (Caviplace laboratory at INRA Bordeaux; Cochard *et al.*, 2005), within 3 wk after sampling. These measurements were used to estimate the hydraulic vulnerability thresholds at which 50% or 88% of conductivity of a branch is lost due to embolism formation. An adapted technique was necessary for *Q. petraea* due to the larger vessel length of *c.* 50 cm, where we used a larger branch and a 27 cm diameter rotor. A logistic function was fit through each set of data points per branch (PLC vs xylem water potential; Ψ_{xylem}) and the Ψ_{xylem} at which 50% (P_{50} in MPa) and 88% loss of conductivity (P_{88} in MPa) occurred were recorded as relevant thresholds. For further measurement and processing details, see Dietrich *et al.* (2019). Besides the P_{50} and P_{88} values, the hydraulic safety margin was calculated by defining the minimum midday Ψ_{leaf} per tree.

Stem radius changes (Δd_{stem}) were processed to partition growth (i.e. irreversible radius increments) and water-related components (i.e. reversible stem shrinkage and expansion) using the TREENETPROC R package (Knüsel *et al.*, 2021). This partitioning was performed according to the zero-growth concept (Zweifel *et al.*, 2016), where diameter variations below the preceding maximum stem diameter are considered as periods of tree water deficit (TWD in μm; i.e. a more severe stem shrinkage results in higher TWD), a common proxy for stem dehydration and tree drought stress (Salomón *et al.*, 2022). The TREENETPROC R packages provided tree-specific time series of TWD and daily shrinkage (in μm). During the daylight hours, TWD increases due to transpiration of the tree, whereas during the night TWD decrease mainly depends on the potential of the tree to rehydrate. Therefore, we quantified the daily minimum TWD to isolate the potential for stem rehydration. In most cases, daily minimum TWD is reached just before sunrise and thus represents the predawn TWD conditions (TWD_{pd}) according to Salomón *et al.* (2022). As absolute TWD_{pd} is affected by both the elasticity of the bark tissue and the size of the tree, we had to normalize TWD_{pd} by dividing it by the tree-specific largest daily shrinkage (calculated as the 99th percentile of absolute daily shrinkage values across the monitoring period; Knüsel *et al.*, 2021) to account for differences in absolute TWD_{pd} between trees (resulting unit = μm μm^{-1}). Here, it is assumed that this diurnal radial shrinkage of the flexible stem tissues (e.g. phloem) reflects the tree-specific differences in storage tissue flexibility and size. Analyses were restricted to data from May until September when stem radius changes and the related physiological processes are mainly affected by transpiration (and not due to phloem collapse in winter or temperature-induced swelling). One *Q. petraea* tree was removed from the analyses (QUPE4, Table 1) due to measurement failures, which we could not correct for.

Quantitative wood anatomy of the stem

To contextualize predawn stem rehydration potential, quantitative wood anatomical analyses were performed to calculate species-specific theoretical hydraulic resistance of the stem's sapwood (samples taken from wood cores described previously). For each wood core, 12-μm-thick cross sections were cut from the sapwood using a rotatory microtome (Leica RM2245; Leica Biosystems, Nussloch, Germany) and prepared according to standard protocol (as described in Prendin *et al.*, 2018). Digital images of the sections (resolution = 2.27 pixel μm^{-1}) were taken using a slide scanner (Axio Scan Z1; Carl Zeiss AG, Oberkochen, Germany). ROXAS (von Arx & Carrer, 2014) was used to measure the lumen size of conductive cells from the collected images. For the entire sapwood depth (Table 1), an adjusted version of the RAPTOR R package (Peters *et al.*, 2018) was used to obtain the theoretical xylem-specific conductivity (K_s in m^2 MPa^{-1} s^{-1}) and the theoretical hydraulic conductance (K_h in m^4 MPa^{-1} s^{-1}) for the xylem area of the sapwood according to the Hagen–Poiseuille law (Tyree & Zimmermann, 2002; Prendin *et al.*, 2018). Here, the hydraulic resistance in the xylem (R_h in MPa s m^{-4}; Eqn 2) of a capillary tube is defined by its length (l, set to 1 m) and lumen diameter (d_{lum}), with η being the dynamic viscosity of water (0.001 Pa S at 20°C). R_s ($1/K_s$) was used to quantify the hydraulic resistance per unit sapwood area.

$$R_h = \frac{128\eta l}{\pi \sum d_{lum}^4} \qquad \text{Eqn 2}$$

Data analyses and statistics

We used the NLME and LME4 R packages (Bates *et al.*, 2015; Pinheiro *et al.*, 2016) to perform linear mixed effect modelling. We assessed all assumptions for each model fit, including normality, heteroscedasticity and independence. We also performed variable transformations where needed (Zuur *et al.*, 2010).

We square rooted the dependent variable G_c/G_{cmax} (to obtain normality and Weibull-shaped response curves; Anderegg *et al.*, 2017) and related this to Ψ_{leaf} and species as fixed effects, while using tree as a random intercept in NLME. The significance of slopes (expressed with λ) and intercepts ($P < 0.05$) were obtained with the EMMEANS R package (Lenth, 2022), while the back-transformed species-specific slopes at 50% conductance loss (expressed as λG_{c50}) and the Ψ_{leaf} at G_{c50} were obtained by using the sim function from the ARM R package (simulations = 1000; Gelman & Su, 2021).

The effect of species on P_{50} and P_{88} was tested using linear models, as was done for analysing species-specific differences in

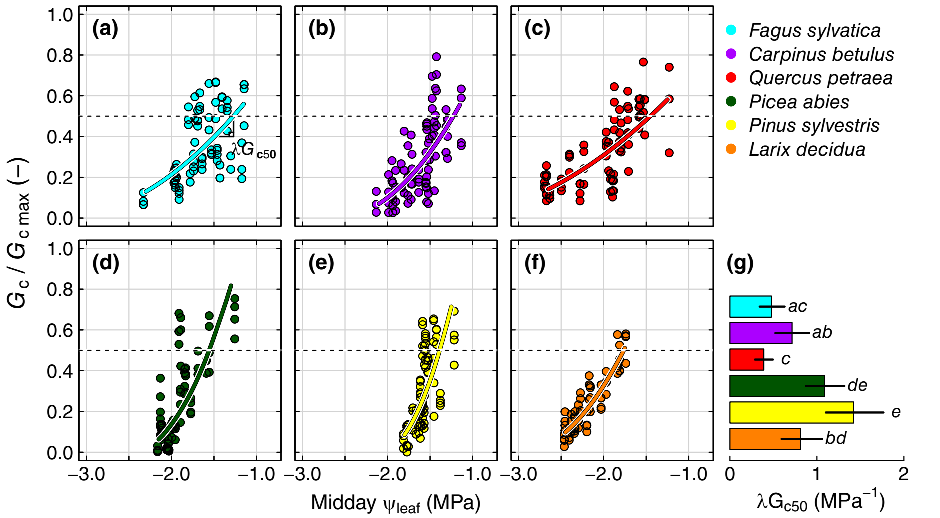

Fig. 2 Response of standardized canopy conductance (G_c/G_{cmax}) to midday leaf water potential (Ψ_{leaf}). (a–f) The input data for the mixed effect model and the fitted mean response are presented for all six species (colour-coded). The horizontal dashed line indicates where 50% of the canopy conductance is lost. An example is provided of how we established the slope at 50% of canopy conductance (λG_{c50} in a). (g) Bars present the species-specific differences in stomatal control, expressed as λG_{c50}, with letters indicating significant differences among species ($P < 0.05$) and error bars presenting the 95% confidence interval of the model.

R_h and R_s. To validate the use of the average Ψ_{soil} dynamics measured at 20 cm depth when considering the rehydration dynamics (H2), we analysed the relationship between predawn Ψ_{leaf} and Ψ_{soil} (see Fig. S1 for other depths). This relationship was modelled per species using NLME with predawn Ψ_{leaf} as a dependent variable, the second-order polynomial Ψ_{soil} as a fixed effect and tree as a random intercept. Wet and dry conditions (dry = Ψsoil < −0.5 MPa) were tested for significant differences between species using emmeans. Predawn stem shrinkage response to drought was analysed by averaging TWD_{pd} values into 0.03 MPa Ψ_{soil} bins per tree species (i.e. to reduce the impact of temporal autocorrelation) to assess the severity of sustained shrinkage during the night, which relates to hampered predawn rehydration. A third-order polynomial structure was given to Ψ_{soil} as a fixed effect with species to explain TWD_{pd}. The tree was added as a random intercept, and a correction was included to account for the discrepancy in absolute variance between species (applying weights with the constant variance function in LME4). Relationships between previously assessed slopes (expressed in λ) and intercepts were performed on the species mean using simple linear models to test the hypotheses.

Results

Stomatal response in relation to midday leaf water potentials

The relationship between G_c/G_{cmax} and midday Ψ_{leaf} presented in Fig. 2(a–f) was captured by the expected Weibull behaviour. It showed species-specific differences, where the three conifers showed significantly steeper slopes compared with the three broadleaf species ($P < 0.001$). Additionally, conifers appeared to have significantly higher intercepts ($P = 0.001$), which is reflected in the more negative midday Ψ_{leaf} at G_{c50} (Fig. 2d–f). The steepest slope at G_{c50}, expressed in λG_{c50} in Fig. 2(g), was found for *P. sylvestris* ($\lambda G_{c50} = 1.42$ MPa^{-1}) that is significantly different from the lowest slopes found for *Q. petraea* ($\lambda G_{c50} = 0.39$ MPa^{-1}; $P < 0.001$). *F. sylvatica* and *Q. petraea* showed no significant difference in λG_{c50} ($P = 0.856$), as was the case for *P. abies* and *P. sylvestris* ($P = 0.217$). The order of species in terms of reduction of canopy conductance in relation to midday Ψ_{leaf}, expressed in λG_{c50}, from the largest to the smallest value was as follows: *P. sylvestris* > *P. abies* > *L. decidua* > *C. betulus* > *F. sylvatica* > *Q. petraea*.

Species-specific percentage loss of conductance in branches

The P_{50} and P_{88} values differed significantly among species (Table 2). The absolute values and species-specific difference matched with P_{50} values reported in the literature (see Kahmen *et al.*, 2022). Both *C. betulus* and *Q. petraea* showed the most negative P_{50} and P_{88} values, with no significant difference between them ($P = 0.910$). *P. sylvestris*, *L. decidua* and *F. sylvatica* showed the least negative P_{50} and P_{88} values, with also no significant difference between them ($P > 0.05$; see Fig. S2 for a detailed overview). *Picea abies* tended to be between these two groups in terms of P_{50} and P_{88} values, yet no significant difference was found.

Predawn leaf water potential relations to soil drought

The predawn Ψ_{leaf} collected in 2015 decreased across all species with decreasing Ψ_{soil} measured at 20 cm depth (Fig. 3a). The second-order polynomial relationship with Ψ_{soil} (Fig. 3b) was significant ($P < 0.001$), with significant differences between species ($P = 0.001$). Additional measurements of Ψ_{soil} in 2015 at 40 and 60 cm depth confirmed that the dynamics measured at 20 cm depth appropriately explained predawn Ψ_{leaf} dynamics (Fig. S1). Predawn Ψ_{leaf} appeared to stabilize with $\Psi_{soil} > -0.5$ MPa, which we considered to be moderately 'wet' conditions, where predawn Ψ_{leaf} did not substantially respond to the drought. From the model fit, the slope of Ψ_{leaf} to Ψ_{soil} during conditions < −0.5 MPa (hence referred to as 'dry') was used to assess the magnitude of the linear response towards soil drying. The slope strongly depended on the species, where *P. abies* and *C. betulus* showed the steepest slopes (2.03 and 1.91 MPa MPa^{-1},

Table 2 P_{50} and P_{88} values measured on the branches of the six monitored species.

Species	P_{50} (MPa)	CI (MPa)		P_{88} (MPa)	CI (MPa)	
Fagus sylvatica	−3.78[c]	−4.11	−3.45	−4.54[c]	−5.05	−4.02
Carpinus betulus	−4.71[ab]	−5.07	−4.34	−5.80[ab]	−6.37	−5.22
Quercus petraea	−5.01[b]	−5.53	−4.49	−6.50[b]	−7.31	−5.69
Picea abies	−4.00[ac]	−4.33	−3.67	−4.84[ac]	−5.36	−4.33
Pinus sylvestris	−3.48[c]	−3.91	−3.05	−4.60[ac]	−5.27	−3.94
Larix decidua	−3.58[c]	−3.91	−3.25	−4.43[c]	−4.94	−3.91

The model mean of the Ψ_{xylem} at which 50% and 88% of the conductance is lost (P_{50} and P_{88}, respectively) and the 95% confidence interval (CI) are provided. Significant differences between species are indicated with letters ($P < 0.05$).

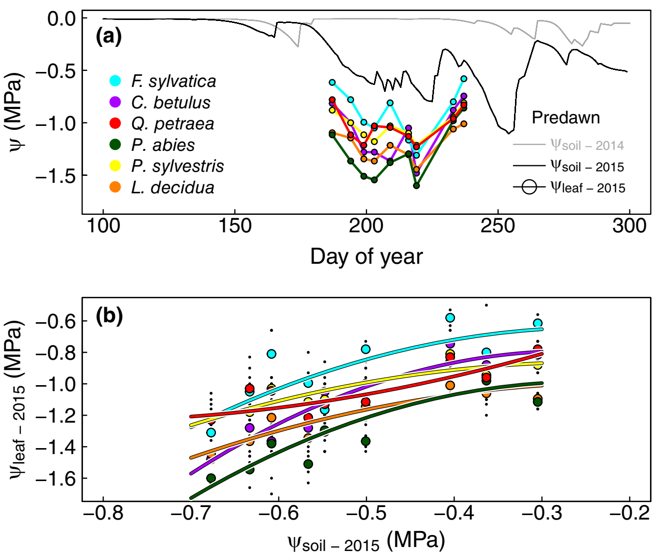

Fig. 3 Relationship between predawn leaf water potential (Ψ_{leaf}) and soil water potential (Ψ_{soil}) at 20 cm depth. (a) Time series of Ψ_{soil} and predawn Ψ_{leaf} for 2015 and Ψ_{soil} measured in 2014 as reference. For each sampling day of the year, the median of each species is presented with coloured dots. (b) Predawn Ψ_{leaf} per species from 2015 was plotted against the corresponding 2015 Ψ_{soil} values. The linear mixed effect model fit is presented with the bold line for each species. The larger filled dots indicate the species-specific median (colours indicate the species as presented in a). The smaller black dots show the raw measurements.

respectively; $P < 0.001$). The smallest slope was found for *Q. petraea* and *P. sylvestris* (0.96 and 1.03 MPa MPa^{-1}, respectively; $P < 0.001$). The slope of *F. sylvatica* (1.63 MPa MPa^{-1}) was comparable to those of *C. betulus* and *P. abies*, whereas that of *L. decidua* (1.19 MPa MPa^{-1}) was similar to *P. sylvestris.*

Predawn stem rehydration

All species showed the expected diurnal cycle of night-time stem swelling and daytime shrinking during high and low Ψ_{soil} conditions (Fig. S3). The smallest diurnal shrinkage was found for *F. sylvatica* and *C. betulus.* By contrast, *L. decidua* and *P. abies* showed the largest maximum difference between midday and predawn Δd_{stem}. Conifers more rapidly increased TWD_{pd} with decreasing

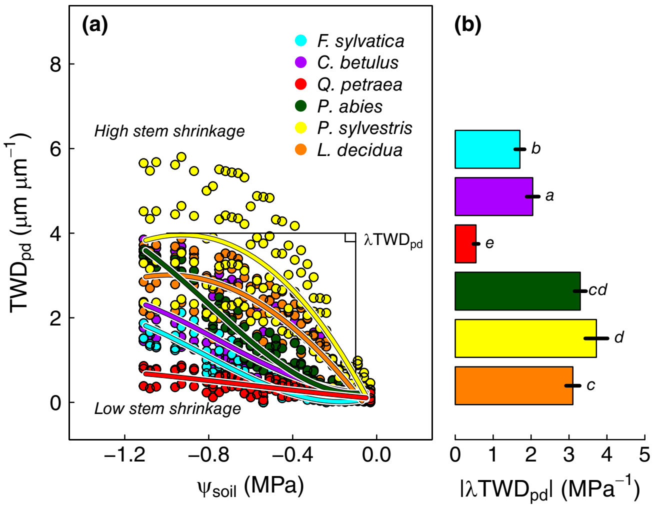

Fig. 4 Response of stem rehydration potential, expressed as predawn tree water deficit (TWD_{pd}; normalized to the maximum daily shrinkage per tree) against daily mean soil water potential (Ψ_{soil}) for the six monitored species. (a) For each species, the fitted mean response line is plotted on the mean TWD_{pd} data point per 0.03 Ψ_{soil} bin for each tree. (b) The absolute slope of the linear part of the TWD_{pd} relationship to Ψ_{soil} (at −0.1 until −1.0 MPa) is plotted, as $|\lambda TWD_{pd}|$ per species (or stem shrinkage rate). Absolute slope values (i.e. none-negative values) are presented to facilitate interpretation – that is, species positioned to the right show a stronger predawn stem shrinkage rate with decreasing Ψ_{soil}. The bars provide the model mean per species, with black lines indicating the subsequent 95% confidence interval. Significant differences between species are indicated with letters.

Ψ_{soil} than broad-leaved species (Fig. 4a), with *P. sylvestris* showing the highest level of TWD_{pd}. The lowest TWD_{pd} among the broad-leaved species was observed for *Q. petraea*, followed by *F. sylvatica* and *C. betulus.* The absolute slope of TWD_{pd} with decreasing Ψ_{soil} at Ψ_{soil} conditions where the relationship becomes linear (−0.1 to −1.0 MPa; Fig. 4b), $|\lambda TWD_{pd}|$ (i.e. the stem shrinkage rate), was the lowest for *Q. petraea* (0.54 MPa^{-1}; $P < 0.001$). The largest response of $|\lambda TWD_{pd}|$ was found for *P. sylvestris* (3.72 MPa^{-1}), which was not significantly different from *P. abies* (2.37 MPa^{-1}; $P = 0.117$). *Picea abies* appeared to have the strongest stem shrinkage increase, followed by *F. sylvatica* and *C. betulus* (Fig. 4a), when analysing the stem shrinkage rates during relatively dry conditions ($\Psi_{soil} < -0.5$ MPa in Fig. 4a). These species also appeared to be the only ones where the $|\lambda TWD_{pd}|$ was significantly steeper ($P < 0.05$) during dry conditions compared with the overall slope (with Ψ_{soil} ranging from −0.1 to −1.0 MPa).

Priorities for reducing stomatal conductance

Species-specific means of λG_{c50}, P_{50} and $|\lambda TWD_{pd}|$ were combined to assess the two hypotheses put forward in Fig. 1 (Fig. 5a, b). For H1, the species-specific behaviour of λG_{c50} showed no significant linear relationship with P_{50} ($P = 0.196$; Fig. 5a) or P_{88} ($P > 0.05$), although the expected positive trend was found, with *P. sylvestris* having the highest P_{50} and conductance regulation. Moreover, P_{50} (and P_{88}) was also not strongly related to the Ψ_{leaf} value at which 50% of the conductance is lost (G_{c50}; $P = 0.503$).

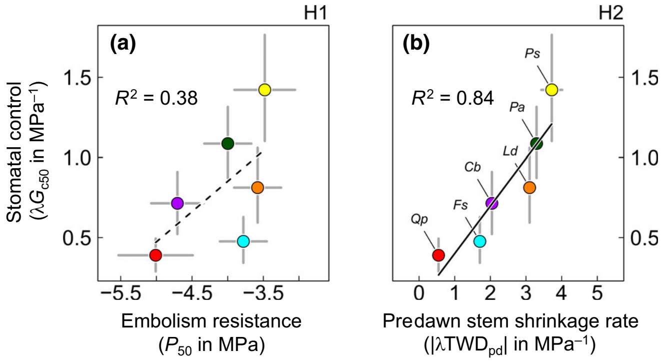

Fig. 5 Linear relationships between species-specific reduction of canopy conductance (λG_{c50}; as presented in Fig. 2g) and the processes hypothesized in Fig. 1. (a) Relationship between λG_{c50} and P_{50} (as presented in Table 2), for testing H1, (b) λG_{c50} and |λTWD$_{pd}$| values (as presented in Fig. 4b), for testing H2. Dashed lines indicate nonsignificant trends, while solid lines indicate significant linear relationships ($P < 0.05$). Species included within these analyses are Ps, *P. sylvestris*; Pa, *P. abies*; Ld, *L. decidua*; Cb, *C. betulus*; Fs, *F. sylvatica* and Qp, *Q. petraea* and are colour-coded in (b). Goodness-of-fit (R^2) of the linear model is provided for both (a, b).

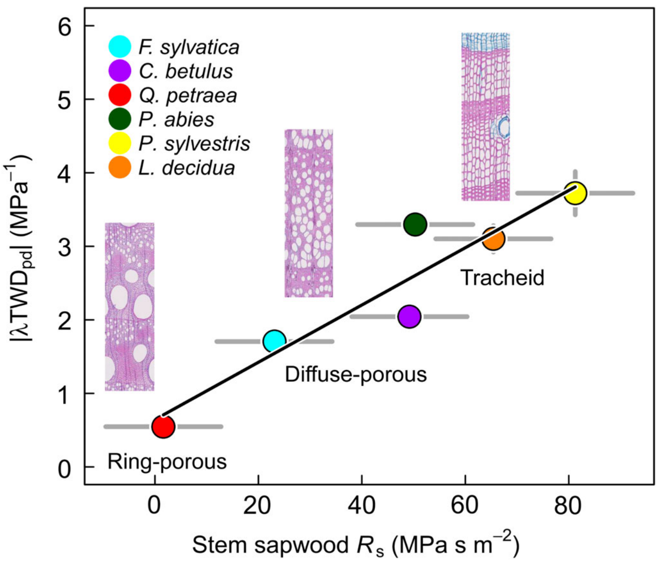

Fig. 6 Linear relationship between species-specific predawn tree water deficit (TWD$_{pd}$) response to Ψ_{soil} (|λTWD$_{pd}$|) and the theoretical xylem-specific hydraulic resistance assessed in the stem sapwood (R_s; Supporting Information Fig. S5). The dots represent the species-specific model mean, and the grey lines show the 95% confidence interval. The significant linear relationship ($P < 0.05$) is presented with a black line.

We found similar results using the hydraulic safety margins as predictive variables for λG_{c50} (Fig. S4). In contrast, λG_{c50} was significantly related to predawn stem shrinkage rate, with increasing |λTWD$_{pd}$| relating to increasing λG_{c50} (intercept = 0.104 and slope = 0.297; $P = 0.011$; Fig. 5b) and supporting H2.

Wood anatomical structure and stem rehydration

The theoretical xylem-specific resistance (R_s) assessed in the stem sapwood as derived from the wood anatomical analyses (*x*-axis in Fig. 6) showed significant differences among species ($P < 0.001$). Ring-porous *Q. petraea* showed the lowest R_s of 1.63 MPa s m^{-2} ($P < 0.001$), followed by diffuse-porous *F. sylvatica* and *C. betulus*. Tracheid-bearing *P. abies* showed similar intermediate R_s values ($P = 0.999$), as did *L. decidua* and *P. sylvestris*, with the highest value ($P = 0.327$). When considering the entire sapwood for calculating the theoretical hydraulic resistance (R_h; Fig. S5), the difference in R_h between *Q. petraea* and *F. sylvatica* disappeared ($P = 0.999$). Most notable is the shift of *L. decidua* that shows the highest R_h value compared with the other species ($P <$ 0.001), while for R_s it is similar to *P. sylvestris*. Notwithstanding, the general R_s and R_h rankings from high to lower values appear similar. Based on these patterns, we could well explain the interspecific differences in |λTWD$_{pd}$|, especially with R_s ($P = 0.021$; Fig. 6), where species with a high R_s have more difficulty rehydrating when water availability is low.

Discussion

We show the variability in tree species-specific reduction of canopy conductance in response to lower water availability (expressed as λG_{c50}). Our main focus was on whether λG_{c50} is prioritizing the avoidance of branch hydraulic failure or rather facilitates predawn stem rehydration. The latter would allow sufficient turgor pressure within the growing tissue at night (Zweifel *et al.*, 2021). Our results provide strong evidence that mature trees in temperate environments are more likely to exhibit stronger stomatal control to facilitate predawn stem rehydration, rather than solely avoiding hydraulic failure in the canopy. As such, we argue that it is important to consider hydraulic processes upstream from the leaves (i.e. towards the roots) and include processes affecting whole-tree internal water pools (i.e. the stem's bark tissue), to better explain responses of mature trees to reduced soil water availability.

Stomatal control, branch xylem vulnerability and predawn stem rehydration

The studied conifer and broadleaf tree species showed distinct differences in G_c response to declining Ψ_{leaf}, where conifers showed a stronger reduction of G_c with decreasing Ψ_{leaf} (i.e. a higher λG_{c50} in Fig. 1a) compared with broadleaves (Fig. 2g). This is consistent with ecosystem-level flux-tower observations (Gharun *et al.*, 2020). The species-specific ranking in λG_{c50} followed our expectation, with *Q. petraea* being more anisohydric than *P. sylvestris* (Aranda *et al.*, 2005; Martínez-Sancho *et al.*, 2017a; Kahmen *et al.*, 2022). This ranking did however not fully support that species with lower branch xylem embolism resistance (expressed in branch P_{50}) consistently show a steeper λG_{c50} (H1 in Fig. 5a). We also did not find a significant positive relationship between P_{50} and G_{c50} ($P = 0.503$), although this relationship was found previously across a broader range of species (Klein, 2014; Henry *et al.*, 2019). Our results furthermore contrast with the theory presented by Joshi *et al.* (2022) that supported the central importance of xylem vulnerability in steering stomatal control in juvenile plants. The discrepancy between our and their findings underlines the difficulty of upscaling such model results based on juvenile trees to mature trees. We hypothesize that, although the efficiency-safety paradigm for stomatal behaviour can be found across larger biomes and species ranges (see Martin-StPaul *et al.*, 2017; Anderegg *et al.*, 2018; Flo *et al.*, 2021), not all mature members of temperate tree species need to prioritize λG_{c50} to avoid branch embolism as they rarely experience extreme drought (i.e. Dietrich *et al.*, 2019; Dietrich & Kahmen, 2019). In other words, temperate trees do not solely prioritize stomatal control to avoid embolism formation.

A strong relationship was found between independent measurements of predawn stem shrinkage dynamics and λG_{c50} (Fig. 5b). To our knowledge, we show here for the first time that the response of G_c appears to be tuned to allow sufficient time for night-time replenishment of stem-water pools (e.g. see Fig. S3) that are used during the day (H2 in Fig. 1b). Species like *P. sylvestris* with their lower hydraulic conductance have greater difficulty to rehydrate their stems during drier conditions and thus impose the strictest stomatal regulation. Allowing the stem bark tissue to relax sufficiently, facilitated by the timely closure of stomata, is critical for building up sufficient turgor pressure within the cambium to allow for growth, which usually happens at night (Peters *et al.*, 2021b; Zweifel *et al.*, 2021; Potkay & Feng, 2022). However, the reduction of G_c means in turn that also the assimilation rate is reduced during the day (Cowan & Farquhar, 1977; Medlyn *et al.*, 2011). Moreover, outside of the time period when radial growth occurs (see Etzold *et al.*, 2022), water flow from the phloem tissue due to transpiration demands can also reduce the efficiency at which sugars are transported down from the canopy (De Schepper & Steppe, 2010; Lemoine *et al.*, 2013; Salmon *et al.*, 2019; Hubau *et al.*, 2020). The loss of turgor within the cambium is known to be affected by both the capacitance of the bark tissue (Zweifel *et al.*, 2006; Salomón *et al.*, 2017) and the hydraulic resistance of the xylem tissue (see Fig. S5; Steppe *et al.*, 2006; Steppe & Lemeur, 2007). We thus find that tree species with a higher stem xylem-specific hydraulic resistance (R_s) exhibit more difficulty with night-time rehydration (Fig. 6) because tracheids do not allow for rapid refilling of the living bark tissue. This finding is critical for explaining the pattern found by Salomón *et al.* (2022), where conifers also showed a relatively higher normalized TWD_{pd} during the 2018 drought across Europe compared with broad-leaved species. We thus conclude that, for understanding stomatal conductance regulation, it is critical to include this 'rehydration-efficiency' trade-off next to considering branch embolism resistance (Zweifel *et al.*, 2007; Henry *et al.*, 2019; Joshi *et al.*, 2022).

Although we find a link between stem rehydration-efficiency and stomatal control, this does not exclude critical structural traits contributing to this relationship. Besides the abovementioned R_s and the impact of the hydraulic architecture (Koch *et al.*, 2004), one theory stresses the importance of the root–soil continuum for stomatal control. Carminati & Javaux (2020) suggested that stomata close when Ψ_{soil} around the roots drops more rapidly than the increase in transpiration (see also Carminati *et al.*, 2020; Rodriguez-Dominguez & Brodribb, 2020; Abdalla *et al.*, 2021), which suggests that species with a less extensive rooting system and a higher R_s have more issues rehydrating their stem tissues. Although we cannot directly assess the efficiency of the root–soil continuum, we expect that stomatal control is unlikely to be solely optimized for soil–root connectivity. The reason for this assumption is that *P. abies*, *C. betulus* and to a lesser extent *F. sylvatica* appear to show a stronger decrease in predawn Ψ_{leaf} with more negative Ψ_{soil} conditions (Fig. 3b), matching well with their root-water uptake in shallower soil depths (Brinkmann *et al.*, 2018; Kahmen *et al.*, 2021; Walthert *et al.*, 2021). However, these species are not consistently the species that show the strongest λG_{c50}, which is likely due to the effects of the hydraulic architecture and storage capacitance (as described previously). Moreover, the relationship shown in Fig. 5(b) does not provide a direct mechanistic link, as the mechanisms for stomatal closure are likely regulated by hormonal signalling in the leaves (i.e. ABA; Brodribb *et al.*, 2014; McAdam & Brodribb, 2014; McAdam *et al.*, 2016), which might have adjusted their response thresholds to facilitate turgor pressure relief.

Drought performance is not well explained by stomatal behaviour alone

Although it is clear that the 2015 drought did not cause any severe mortality risks to the monitored individuals at the site investigated here (Dietrich *et al.*, 2019), a similar Swiss temperate forest site nearby clearly showed a higher mortality risk for *P. abies* (Arend *et al.*, 2021) and postdrought foliage reduction for *F. sylvatica* during and after the 2018 drought (Schuldt *et al.*, 2020; Arend *et al.*, 2022; Kahmen *et al.*, 2022). Surprisingly, these species do not show consistently less negative P_{50} values (Table 2). Besides mortality risks due to hydraulic failure (McDowell *et al.*, 2008), the performance of a tree during drought (i.e. low soil water availability) can also be classified with radial growth sensitivity to drought, as this is the first process to be downregulated when water availability becomes scarce (Peters *et al.*, 2021b; Zweifel *et al.*, 2021; Krejza *et al.*, 2022). A climate-tree-ring-width correlation analysis (e.g. Peters *et al.*, 2017), performed on the sampled trees at the studied site, revealed that particularly *P. abies*, *F. sylvatica* and *C. betulus* show a positive correlation with current-year precipitation and a negative relationship with temperature (Fig. S6; with climate data from Harris *et al.*, 2020). Moreover, both late-successional species *F. sylvatica* and *P. abies* are known to be drought sensitive in their productivity (Babst *et al.*, 2013; Trotsiuk *et al.*, 2020), which is further exemplified by strongly reduced gross primary productivity of beech- and spruce-dominated forests during the 2018 summer drought (Gharun *et al.*, 2020). This indicates a long-term impact of drought on the growth for these species and to a lesser extent for *L. decidua*, *Q. petraea* and *P. sylvestris*. However, at different sites, *P. sylvestris* was also found to be heavily impacted by the 2018 drought, likely due to its occurrence of well-drained sandy soils in other areas (Schuldt *et al.*, 2020). This ranking of drought vulnerability is not consistent with the λG_{c50} patterns found in our study (Fig. 2g), where *Q. petraea*, in contrast to *P. sylvestris*, showed lower stomatal control with lower water availability.

Our results support that λG_c is likely constrained by $|\lambda TWD_{pd}|$ (Fig. 5b), which depends on R_s (Fig. 6) and thus on stricter stomatal control. This probably relates to the water residence times within the tree. For instance, compared with the other studied species, *P. sylvestris* has a longer water residence time in the bark due to its slower refilling (owed to its xylem structure; Fig. 6), higher storage water use (Fig. 4a) and stronger stomatal control (Fig. 2e). This is confirmed by the study of Kahmen *et al.* (2021) where a ^{2}H pulse labelling experiment of the soil water revealed that species like *P. sylvestris* take longer to show the label within the crown. When considering growth sensitivity to drought (see Fig. S6), the abovementioned species ranking in terms of drought performance mainly matches the $|\lambda TWD_{pd}|$ dynamics during drier soil conditions (i.e. *P. abies*, *F.* sylvatica and *C. betulus* continue to shrink compared with the other species in Fig. 4a) when stomatal closure is already approached. Such findings emphasize that it might be misleading to solely use stomatal control when assessing species-specific drought performance (as suggested by Martínez-Vilalta & Garcia-Forner, 2017).

Critical considerations and future prospects

The hydraulic mechanisms identified in this study were standardized to the organ level (i.e. G_c), as it remains challenging to scale the results to the whole-tree level (Martínez-Vilalta *et al.*, 2009; Greenwood *et al.*, 2017; Mencuccini *et al.*, 2019a,b). Especially, tissue properties have been shown to change over longer periods of time when drought persists (i.e. adjustments in leaf and sapwood area; Martínez-Sancho *et al.*, 2017b; Novick *et al.*, 2019; Zweifel *et al.*, 2020). One key limiting factor in xylem vulnerability studies is that branch embolism resistance might not represent the entire living individual appropriately (McCulloh *et al.*, 2014, 2019). Although terminal branch embolism vulnerability has been linked to drought-induced mortality (e.g. for *P. abies*; Arend *et al.*, 2022), multiple studies have shown that whole-tree embolism resistance might depend on root xylem vulnerability (e.g. Domec *et al.*, 2010; Peters *et al.*, 2020) and that the embolism resistance of different xylem tissues might change with age or size of the tree (e.g. Domec & Gartner, 2003; Domec *et al.*, 2009). As such, there is a need to incorporating more xylem tissues for fully elucidating the whole-tree embolism resistance. Another scaling issue revolves around the analyses of tree hydraulic responses to changing Ψ_{soil} measured at a single depth. Although in this study we confirmed that our trees are most responsive to shallower soil depths, the consideration of multiple depths is critical in forest ecosystems where trees might respond to soil moisture dynamics in deeper soil layers due to more severe droughts or vertically more extensive rooting systems.

Notwithstanding, our analyses provide a way forward in quantifying species-specific stomatal control and identifying the complementary hydraulic mechanisms that can explain drought sensitivity within the environmental context (as proposed by Feng *et al.*, 2018). Previous studies have confirmed that tree species have different capacities in adjusting their leaf stomatal apparatus (Poyatos *et al.*, 2007; Grossiord *et al.*, 2017; Peters *et al.*, 2019; Gagne *et al.*, 2020; Bachofen *et al.*, 2023), leaf traits (Rosas *et al.*, 2019) and wood anatomical features (Fonti & Jansen, 2012; Martínez-Sancho *et al.*, 2017a,b) to their respective environment. The utility of our proposed approach to test the raised hypotheses will thus fully unfold once more tree-specific measurements are explored across broad environmental gradients to evaluate intraspecific variability (i.e. phenotypic plasticity or adaptation) of hydraulic traits. Moreover, confirming that stomatal control indeed prioritizes stem rehydration over reducing branch embolism formation as a general rule will require studying a greater diversity of tree species and sites. Nonetheless, our results reveal that mechanistic models on stomatal control need to consider stem-water storage, hydraulic capacitance and turgor-dependent growth processes to fully explain species-specific differences in drought-induced stomatal control and complement the safety–efficiency paradigm.

Acknowledgements

RLP acknowledges the support of the Swiss National Science Foundation (SNSF), Grant P2BSP3_184475. MG acknowledges funding by Swiss National Science Foundation Project ICOS-CH Phase 3 20FI20_198227. FB acknowledges funding from the project 'Inside out' (#POIR.04.04.00-00-5F85/18-00) funded by the HOMING programme of the Foundation for Polish Science co-financed by the European Union under the European Regional Development Fund. LD acknowledges the support provided by the Department of Environmental Sciences at the University of Basel and the Swiss Federal Office for the Environment (FOEN). RP acknowledges support by the grant RTI2018-095297-J-I00 (Spain). CG acknowledges funding by the Swiss National Science Foundation (310030_204697). We would also like to thank three anonymous reviewers for their generous time in providing detailed comments and suggestions, which helped us to improve the presented research.

Competing interests

None declared.

Author contributions

RLP, KS and AK designed the study. Discussions among all authors contributed to its subsequent conceptual and theoretical development. Data collection was performed by LD, MF, RLP and AK. RLP and CP developed the analyses framework and wrote the first draft of the manuscript with aid from FB, KS and AK, to which RZ, LD, GvA, RP, MF, PF, CG, MG, NB and DNS contributed revisions. Funding was obtained by RLP with the aid of AK and KS.

ORCID

Georg von Arx https://orcid.org/0000-0002-8566-4599
Flurin Babst https://orcid.org/0000-0003-4106-7087
Nina Buchmann https://orcid.org/0000-0003-0826-2980

Lars Dietrich https://orcid.org/0000-0003-3407-166X
Marina Fonti https://orcid.org/0000-0002-2415-8019
Patrick Fonti https://orcid.org/0000-0002-7070-3292
Mana Gharun https://orcid.org/0000-0003-0337-7367
Charlotte Grossiord https://orcid.org/0000-0002-9113-3671
Ansgar Kahmen https://orcid.org/0000-0002-7823-5163
Christoforos Pappas https://orcid.org/0000-0001-5721-557X
Richard L. Peters https://orcid.org/0000-0002-7441-1297
Rafael Poyatos https://orcid.org/0000-0003-0521-2523
Kathy Steppe https://orcid.org/0000-0001-6252-0704
David N. Steger https://orcid.org/0000-0001-7410-0010
Roman Zweifel https://orcid.org/0000-0001-9438-0582

Data availability

The data that support the findings of this study are available on the Dryad Digital Repository doi: 10.5061/dryad.25b8k25.

References

Abdalla M, Carminati A, Cai G, Javaux M, Ahmed MA. 2021. Stomatal closure of tomato under drought is driven by an increase in soil–root hydraulic resistance. *Plant, Cell & Environment* **44**: 425–431.

Anderegg WRL, Tamir K, Megan B, Lawren S, Pellegrini AFA, Brendan C, Steven J. 2016. Meta-analysis reveals that hydraulic traits explain cross-species patterns of drought-induced tree mortality across the globe. *Proceedings of the National Academy of Sciences, USA* **113**: 5024–5029.

Anderegg WRL, Wolf A, Arango-Velez A, Choat B, Chmura DJ, Jansen S, Kolb T, Li S, Meinzer F, Pita P *et al.* 2017. Plant water potential improves prediction of empirical stomatal models. *PLoS ONE* **12**: e0185481.

Anderegg WRL, Wolf A, Arango-Velez A, Choat B, Chmura DJ, Jansen S, Kolb T, Li S, Meinzer FC, Pita P *et al.* 2018. Woody plants optimise stomatal behaviour relative to hydraulic risk. *Ecology Letters* **21**: 968–977.

Aranda I, Gil L, Pardos JA. 2005. Seasonal changes in apparent hydraulic conductance and their implications for water use of European beech (*Fagus sylvatica* L.) and sessile oak [*Quercus petraea* (Matt.) Liebl] in South Europe. *Plant Ecology* **179**: 155–167.

Arend M, Link RM, Patthey R, Hoch G, Schuldt B, Kahmen A. 2021. Rapid hydraulic collapse as cause of drought-induced mortality in conifers. *Proceedings of the National Academy of Sciences, USA* **118**: e2025251118.

Arend M, Link RM, Zahnd C, Hoch G, Schuldt B, Kahmen A. 2022. Lack of hydraulic recovery as a cause of post-drought foliage reduction and canopy decline in European beech. *New Phytologist* **234**: 1195–1205.

von Arx G, Carrer M. 2014. ROXAS: a new tool to build centuries-long tracheid-lumen chronologies in conifers. *Dendrochronologia* **32**: 290–293.

Babst F, Bouriaud O, Poulter B, Trouet V, Girardin MP, Frank DC. 2019. Twentieth century redistribution in climatic drivers of global tree growth. *Science Advances* **5**: eaat4313.

Babst F, Poulter B, Trouet V, Tan K, Neuwirth B, Wilson R, Carrer M, Grabner M, Tegel W, Levanic T *et al.* 2013. Site- and species-specific responses of forest growth to climate across the European continent. *Global Ecology and Biogeography* **22**: 706–717.

Bachofen C, Poyatos R, Flo V, Martínez-Vilalta J, Mencuccini M, Granda V, Grossiord C. 2023. Stand structure of Central European forests matters more than climate for transpiration sensitivity to VPD. *Journal of Applied Ecology* **60**: 886–897.

Bartlett MK, Klein T, Jansen S, Choat B, Sack L. 2016. The correlations and sequence of plant stomatal, hydraulic, and wilting responses to drought. *Proceedings of the National Academy of Sciences, USA* **113**: 13098–13103.

Bates D, Mächler M, Bolker B, Walker S. 2015. Fitting linear mixed-effects models using LME4. *Journal of Statistical Software* **67**: 1–48.

Brinkmann N, Eugster W, Buchmann N, Kahmen A. 2018. Species-specific differences in water uptake depth of mature temperate trees vary with water availability in the soil. *Plant Biology* **21**: 71–81.

Brodribb TJ, Holbrook NM. 2004. Stomatal protection against hydraulic failure: a comparison of coexisting ferns and angiosperms. *New Phytologist* **162**: 663–670.

Brodribb TJ, McAdam SAM, Jordan GJ, Martins SCV. 2014. Conifer species adapt to low-rainfall climates by following one of two divergent pathways. *Proceedings of the National Academy of Sciences, USA* **111**: 14489–14493.

Buckley TN. 2019. How do stomata respond to water status? *New Phytologist* **224**: 21–36.

Buras A, Rammig A, Zang CS. 2020. Quantifying impacts of the 2018 drought on European ecosystems in comparison to 2003. *Biogeosciences* **17**: 1655–1672.

Cabon A, Kannenberg SA, Arain A, Babst F, Baldocchi D, Belmecheri S, Delpierre N, Guerrieri R, Maxwell JT, McKenzie S *et al.* 2022. Cross-biome synthesis of source versus sink limits to tree growth. *Science* **376**: 758–761.

Carminati A, Ahmed MA, Zarebanadkouki M, Cai G, Lovric G, Javaux M. 2020. Stomatal closure prevents the drop in soil water potential around roots. *New Phytologist* **226**: 1541–1543.

Carminati A, Javaux M. 2020. Soil rather than xylem vulnerability controls stomatal response to drought. *Trends in Plant Science* **25**: 868–880.

Choat B, Brodribb TJ, Brodersen CR, Duursma RA, López R, Medlyn BE. 2018. Triggers of tree mortality under drought. *Nature* **558**: 531–539.

Cochard H, Damour G, Bodet C, Tharwat I, Poirier M, Améglio T. 2005. Evaluation of a new centrifuge technique for rapid generation of xylem vulnerability curves. *Physiologia Plantarum* **124**: 410–418.

Comstock J, Mencuccini M. 1998. Control of stomatal conductance by leaf water potential in *Hymenoclea salsola* (T. & G.), a desert subshrub. *Plant, Cell & Environment* **21**: 1029–1038.

Coussement JR, Villers SLY, Nelissen H, Inzé D, Steppe K. 2021. Turgor-time controls grass leaf elongation rate and duration under drought stress. *Plant, Cell & Environment* **44**: 1361–1378.

Cowan IR, Farquhar GD. 1977. Stomatal function in relation to leaf metabolism and environment. *Symposia of the Society for Experimental Biology* **31**: 471–505.

Damour G, Simonneau T, Cochard H, Urban L. 2010. An overview of models of stomatal conductance at the leaf level. *Plant, Cell & Environment* **33**: 1419–1438.

Darwin F. 1898. Observations on stomata. *Proceedings of the Royal Society of London* **63**: 413–417.

De Schepper V, Steppe K. 2010. Development and verification of a water and sugar transport model using measured stem diameter variations. *Journal of Experimental Botany* **61**: 2083–2099.

Delzon S, Cochard H. 2014. Recent advances in tree hydraulics highlight the ecological significance of the hydraulic safety margin. *New Phytologist* **203**: 355–358.

Dietrich L, Delzon S, Hoch G, Kahmen A. 2019. No role for xylem embolism or carbohydrate shortage in temperate trees during the severe 2015 drought. *Journal of Ecology* **107**: 334–349.

Dietrich L, Kahmen A. 2019. Water relations of drought-stressed temperate trees benefit from short drought-intermitting rainfall events. *Agricultural and Forest Meteorology* **265**: 70–77.

Domec JC, Gartner BL. 2003. Relationship between growth rates and xylem hydraulic characteristics in young, mature and old-growth ponderosa pine trees. *Plant, Cell & Environment* **26**: 471–483.

Domec JC, Schäfer K, Oren R, Kim HS, McCarthy HR. 2010. Variable conductivity and embolism in roots and branches of four contrasting tree species and their impacts on whole-plant hydraulic performance under future atmospheric CO_2 concentration. *Tree Physiology* **30**: 1001–1015.

Domec JC, Warren JM, Meinzer FC, Lachenbruch B. 2009. Safety factors for xylem failure by implosion and air-seeding within roots, trunks and branches of young and old conifer trees. *IAWA Journal* **30**: 101–120.

Edwards D, Kerp H, Hass H. 1998. Stomata in early land plants: an anatomical and ecophysiological approach. *Journal of Experimental Botany* **49**: 255–278.

Etzold S, Sterck F, Bose AK, Braun S, Buchmann N, Eugster W, Gessler A, Kahmen A, Peters RL, Vitasse Y *et al.* 2022. Number of growth days and not length of the growth period determines radial stem growth of temperate trees. *Ecology Letters* **25**: 427–439.

Fatichi S, Pappas C, Ivanov VY. 2016. Modeling plant–water interactions: an ecohydrological overview from the cell to the global scale. *Wiley Interdisciplinary Reviews: Water* **3**: 327–368.

Fatichi S, Pappas C, Zscheischler J, Leuzinger S. 2019. Modelling carbon sources and sinks in terrestrial vegetation. *New Phytologist* **221**: 652–668.

Feng X, Ackerly DD, Dawson TE, Manzoni S, Skelton RP, Vico G, Thompson SE. 2018. The ecohydrological context of drought and classification of plant responses. *Ecology Letters* **21**: 1723–1736.

Flo V, Martínez-Vilalta J, Mencuccini M, Granda V, Anderegg WRL, Poyatos R. 2021. Climate and functional traits jointly mediate tree water-use strategies. *New Phytologist* **231**: 617–630.

Fonti P, Jansen S. 2012. Xylem plasticity in response to climate. *New Phytologist* **195**: 734–736.

Forrester DI, Tachauer IHH, Annighoefer P, Barbeito I, Pretzsch H, Ruiz-Peinado R, Stark H, Vacchiano G, Zlatanov T, Chakraborty T *et al.* 2017. Generalized biomass and leaf area allometric equations for European tree species incorporating stand structure, tree age and climate. *Forest Ecology and Management* **396**: 160–175.

Gagne MA, Smith DD, McCulloh KA. 2020. Limited physiological acclimation to recurrent heatwaves in two boreal tree species. *Tree Physiology* **40**: 1680–1696.

Gelman A, Su YS. 2021. *ARM: data analysis using regression and multilevel/hierarchical models.* R Package v.1.12-2. [WWW document] URL https://CRAN.R-project.org/package=arm [accessed 15 October 2021].

Gharun M, Hörtnagl L, Paul-Limoges E, Ghiasi S, Feigenwinter I, Burri S, Marquardt K, Etzold S, Zweifel R, Eugster W *et al.* 2020. Physiological response of Swiss ecosystems to 2018 drought across plant types and elevation. *Philosophical Transactions of the Royal Society B: Biological Sciences* **375**: 20190521.

Granier A. 1985. Une nouvelle méthode pour la mesure du flux de sève brute dans le tronc des arbres. *Annals of Forest Science* **42**: 193–200.

Greenwood S, Ruiz-Benito P, Martínez-Vilalta J, Lloret F, Kitzberger T, Allen CD, Fensham R, Laughlin DC, Kattge J, Bönisch G *et al.* 2017. Tree mortality across biomes is promoted by drought intensity, lower wood density and higher specific leaf area. *Ecology Letters* **20**: 539–553.

Grossiord C, Buckley TN, Cernusak LA, Novick KA, Poulter B, Siegwolf RTW, Sperry JS, McDowell NG. 2020. Plant responses to rising vapor pressure deficit. *New Phytologist* **226**: 1550–1566.

Grossiord C, Sevanto S, Borrego I, Chan AM, Collins AD, Dickman LT, Hudson PJ, McBranch N, Michaletz ST, Pockman WT *et al.* 2017. Tree water dynamics in a drying and warming world. *Plant, Cell & Environment* **40**: 1861–1873.

Hammond WM, Williams AP, Abatzoglou JT, Adams HD, Klein T, López R, Sáenz-Romero C, Hartmann H, Breshears DD, Allen CD. 2022. Global field observations of tree die-off reveal hotter-drought fingerprint for Earth's forests. *Nature Communications* **13**: 1761.

Harris I, Osborn TJ, Jones P, Lister D. 2020. Version 4 of the CRU TS monthly high-resolution gridded multivariate climate dataset. *Scientific Data* **7**: 109.

Henry C, John GP, Pan R, Bartlett MK, Fletcher LR, Scoffoni C, Sack L. 2019. A stomatal safety-efficiency trade-off constrains responses to leaf dehydration. *Nature Communications* **10**: 3398.

Hochberg U, Rockwell FE, Holbrook NM, Cochard H. 2018. Iso/anisohydry: a plant–environment interaction rather than a simple hydraulic trait. *Trends in Plant Science* **23**: 112–120.

Hubau W, Lewis SL, Phillips OL, Affum-Baffoe K, Beeckman H, Cuní-Sanchez A, Daniels AK, Ewango CEN, Fauset S, Mukinzi JM *et al.* 2020. Asynchronous carbon sink saturation in African and Amazonian tropical forests. *Nature* **579**: 80–87.

Hurley AG, Peters RL, Pappas C, Steger DN, Heinrich I. 2022. Addressing the need for interactive, efficient, and reproducible data processing in ecology with the DATACLEANR R package. *PLoS ONE* **17**: e0268426.

Jarvis PG, Monteith JL, Weatherley PE. 1976. The interpretation of the variations in leaf water potential and stomatal conductance found in canopies in the field. *Philosophical Transactions of the Royal Society of London. Series B: Biological Sciences* **273**: 593–610.

Joshi J, Stocker BD, Hofhansl F, Zhou S, Dieckmann U, Prentice IC. 2022. Towards a unified theory of plant photosynthesis and hydraulics. *Nature Plants* **8**: 1304–1316.

Kahmen A, Basler D, Hoch G, Link RM, Schuldt B, Zahnd C, Arend M. 2022. Root water uptake depth determines the hydraulic vulnerability of temperate European tree species during the extreme 2018 drought. *Plant Biology* **24**: 1224–1239.

Kahmen A, Buser T, Hoch G, Grun G, Dietrich L. 2021. Dynamic ^2H irrigation pulse labelling reveals rapid infiltration and mixing of precipitation in the soil and species-specific water uptake depths of trees in a temperate forest. *Ecohydrology* **14**: e2322.

Kannenberg SA, Novick KA, Alexander MR, Maxwell JT, Moore DJP, Phillips RP, Anderegg WRL. 2019. Linking drought legacy effects across scales: from leaves to tree rings to ecosystems. *Global Change Biology* **25**: 2978–2992.

Katul G, Manzoni S, Palmroth S, Oren R. 2010. A stomatal optimization theory to describe the effects of atmospheric CO_2 on leaf photosynthesis and transpiration. *Annals of Botany* **105**: 431–442.

Klein T. 2014. The variability of stomatal sensitivity to leaf water potential across tree species indicates a continuum between isohydric and anisohydric behaviours. *Functional Ecology* **28**: 1313–1320.

Knüsel S, Peters RL, Haeni M, Wilhelm M, Zweifel R. 2021. Processing and extraction of seasonal tree physiological parameters from stem radius time series. *Forests* **12**: 765.

Koch GW, Sillett SC, Jennings GM, Davis SD. 2004. The limits to tree height. *Nature* **428**: 851–854.

Krejza J, Haeni M, Darenova E, Foltýnová L, Fajstavr M, Světlík J, Nezval O, Bednář P, Šigut L, Horáček P *et al.* 2022. Disentangling carbon uptake and allocation in the stems of a spruce forest. *Environmental and Experimental Botany* **196**: 104787.

Lemoine R, La Camera S, Atanassova R, Dédaldéchamp F, Allario T, Pourtau N, Bonnemain J-L, Laloi M, Coutos-Thévenot P, Maurousset L *et al.* 2013. Source-to-sink transport of sugar and regulation by environmental factors. *Frontiers in Plant Science* **4**: 00272.

Lenth RV. 2022. *EMMEANS: estimated marginal means, aka least-squares means.* R Package v.1.7.4-1. [WWW document] URL https://CRAN.R-project.org/package=emmeans [accessed 15 May 2022].

Lu P, Urban L, Ping Z. 2004. Granier's Thermal Dissipation Probre (TDP) method for measuring sap flow in trees: theory and practice. *Acta Botanica Sinica* **46**: 631–646.

Mantova M, Menezes-Silva PE, Badel E, Cochard H, Torres-Ruiz JM. 2021. The interplay of hydraulic failure and cell vitality explains tree capacity to recover from drought. *Physiologia Plantarum* **172**: 247–257.

Martínez-Sancho E, Dorado-Liñán I, Hacke UG, Seidel H, Menzel A. 2017a. Contrasting hydraulic architectures of scots pine and sessile oak at their southernmost distribution limits. *Frontiers in Plant Science* **8**: 1–12.

Martínez-Sancho E, Dorado-Liñán I, Heinrich I, Helle G, Menzel A. 2017b. Xylem adjustment of sessile oak at its southern distribution limits. *Tree Physiology* **37**: 903–914.

Martinez-Vilalta J, Anderegg WRL, Sapes G, Sala A. 2019. Greater focus on water pools may improve our ability to understand and anticipate drought-induced mortality in plants. *New Phytologist* **223**: 22–32.

Martínez-Vilalta J, Cochard H, Mencuccini M, Sterck F, Herrero A, Korhonen JFJ, Llorens P, Nikinmaa E, Nolè A, Poyatos R *et al.* 2009. Hydraulic adjustment of Scots pine across Europe. *New Phytologist* **184**: 353–364.

Martínez-Vilalta J, Garcia-Forner N. 2017. Water potential regulation, stomatal behaviour and hydraulic transport under drought: deconstructing the iso/anisohydric concept. *Plant, Cell & Environment* **40**: 962–976.

Martin-StPaul N, Delzon S, Cochard H. 2017. Plant resistance to drought depends on timely stomatal closure. *Ecology Letters* **20**: 1437–1447.

Mastrotheodoros T, Pappas C, Molnar P, Burlando P, Manoli G, Parajka J, Rigon R, Szeles B, Bottazzi M, Hadjidoukas P *et al.* 2020. More green and less blue water in the Alps during warmer summers. *Nature Climate Change* **10**: 155–161.

McAdam SAM, Brodribb TJ. 2014. Separating active and passive influences on stomatal control of transpiration. *Plant Physiology* **164**: 1578–1586.

McAdam SAM, Manzi M, Ross JJ, Brodribb TJ, Gómez-Cadenas A. 2016. Uprooting an abscisic acid paradigm: Shoots are the primary source. *Plant Signaling & Behavior* **11**: e1169359.

McCulloh KA, Domec J-C, Johnson DM, Smith DD, Meinzer FC. 2019. A dynamic yet vulnerable pipeline: Integration and coordination of hydraulic traits across whole plants. *Plant, Cell & Environment* **42**: 2789–2807.

McCulloh KA, Johnson DM, Meinzer FC, Woodruff DR. 2014. The dynamic pipeline: hydraulic capacitance and xylem hydraulic safety in four tall conifer species. *Plant, Cell & Environment* **37**: 1171–1183.

McDowell N, Pockman WT, Allen CD, Breshears DD, Cobb N, Kolb T, Plaut J, Sperry J, West A, Williams DG *et al.* 2008. Mechanisms of plant survival and mortality during drought: why do some plants survive while others succumb to drought? *New Phytologist* **178**: 719–739.

Medlyn BE, Duursma RA, Eamus D, Ellsworth DS, Prentice IC, Barton CVM, Crous KY, De Angelis P, Freeman M, Wingate L. 2011. Reconciling the optimal and empirical approaches to modelling stomatal conductance. *Global Change Biology* **17**: 2134–2144.

Mencuccini M, Manzoni S, Christoffersen B. 2019a. Modelling water fluxes in plants: from tissues to biosphere. *New Phytologist* **222**: 1207–1222.

Mencuccini M, Rosas T, Rowland L, Choat B, Cornelissen H, Jansen S, Kramer K, Lapenis A, Manzoni S, Niinemets Ü *et al.* 2019b. Leaf economics and plant hydraulics drive leaf: wood area ratios. *New Phytologist* **224**: 1544–1556.

Novick KA, Ficklin DL, Stoy PC, Williams CA, Bohrer G, Oishi AC, Papuga SA, Blanken PD, Noormets A, Sulman BN *et al.* 2016. The increasing importance of atmospheric demand for ecosystem water and carbon fluxes. *Nature Climate Change* **6**: 1023–1027.

Novick KA, Konings AG, Gentine P. 2019. Beyond soil water potential: An expanded view on isohydricity including land–atmosphere interactions and phenology. *Plant, Cell & Environment* **42**: 1802–1815.

Oren R, Sperry JS, Katul GG, Pataki DE, Ewers BE, Phillips N, Schäfer KVR. 1999. Survey and synthesis of intra- and interspecific variation in stomatal sensitivity to vapour pressure deficit. *Plant, Cell & Environment* **22**: 1515–1526.

Pappas C, Matheny AM, Baltzer JL, Barr AG, Black TA, Bohrer G, Detto M, Maillet J, Roy A, Sonnentag O *et al.* 2018. Boreal tree hydrodynamics: asynchronous, diverging, yet complementary. *Tree Physiology* **38**: 953–964.

Peters JMR, Gauthey A, Lopez R, Carins-Murphy MR, Brodribb TJ, Choat B. 2020. Non-invasive imaging reveals convergence in root and stem vulnerability to cavitation across five tree species. *Journal of Experimental Botany* **71**: 6623–6637.

Peters RL, Balanzategui D, Hurley AG, von Arx G, Prendin AL, Cuny HE, Björklund J, Frank DC, Fonti P. 2018. RAPTOR: row and position tracheid organizer in R. *Dendrochronologia* **47**: 10–16.

Peters RL, Klesse S, Fonti P, Frank DC. 2017. Contribution of climate vs larch budmoth outbreaks in regulating biomass accumulation in high-elevation forests. *Forest Ecology and Management* **401**: 147–158.

Peters RL, Pappas C, Hurley AG, Poyatos R, Flo V, Zweifel R, Goossens W, Steppe K. 2021a. Assimilate, process and analyse thermal dissipation sap flow data using the TREX R package. *Methods in Ecology and Evolution* **12**: 342–350.

Peters RL, Speich M, Pappas C, Kahmen A, von Arx G, Graf Pannatier E, Steppe K, Treydte K, Stritih A, Fonti P. 2019. Contrasting stomatal sensitivity to temperature and soil drought in mature alpine conifers. *Plant, Cell & Environment* **42**: 1674–1689.

Peters RL, Steppe K, Cuny HE, De Pauw DJW, Frank DC, Schaub M, Rathgeber CBK, Cabon A, Fonti P. 2021b. Turgor – a limiting factor for radial growth in mature conifers along an elevational gradient. *New Phytologist* **229**: 213–229.

Pinheiro J, Bates D, DebRoy S, Sarkar D, R Core Team. 2016. *NLME: linear and nonlinear mixed effects models.* R Package v.3.1-126. [WWW document] URL http://CRAN.R-project.org/package=nlme [accessed 7 September 2021].

Potkay A, Feng X. 2022. Do stomata optimize turgor-driven growth? A new framework for integrating stomata response with whole-plant hydraulics and carbon balance. *New Phytologist* **238**: 506–528.

Poyatos R, Martínez-Vilalta J, Čermák J, Ceulemans R, Granier A, Irvine J, Köstner B, Lagergren F, Meiresonne L, Nadezhdina N *et al.* 2007. Plasticity in hydraulic architecture of Scots pine across Eurasia. *Oecologia* **153**: 245–259.

Prendin AL, Petit G, Fonti P, Rixen C, Dawes MA, von Arx G. 2018. Axial xylem architecture of *Larix decidua* exposed to CO_2 enrichment and soil warming at the tree line. *Functional Ecology* **32**: 273–287.

R Core Team. 2017. *R: a language and environment for statistical computing.* Vienna, Austria: R Foundation for Statistical Computing. [WWW document] URL https://www.R-project.org/ [accessed 1 April 2023].

Rodriguez-Dominguez CM, Brodribb TJ. 2020. Declining root water transport drives stomatal closure in olive under moderate water stress. *New Phytologist* **225**: 126–134.

Rosas T, Mencuccini M, Barba J, Cochard H, Saura-Mas S, Martínez-Vilalta J. 2019. Adjustments and coordination of hydraulic, leaf and stem traits along a water availability gradient. *New Phytologist* **223**: 632–646.

Salmon Y, Dietrich L, Sevanto S, Hölttä T, Dannoura M, Epron D. 2019. Drought impacts on tree phloem: from cell-level responses to ecological significance. *Tree Physiology* **39**: 173–191.

Salomón RL, Limousin J-M, Ourcival J-M, Rodríguez-Calcerrada J, Steppe K. 2017. Stem hydraulic capacitance decreases with drought stress: implications for modelling tree hydraulics in the Mediterranean oak *Quercus ilex*. *Plant, Cell & Environment* **40**: 1379–1391.

Salomón RL, Peters RL, Zweifel R, Sass-Klaassen UGW, Stegehuis AI, Smiljanic M, Poyatos R, Babst F, Cienciala E, Fonti P *et al.* 2022. The 2018 European heatwave led to stem dehydration but not to consistent growth reductions in forests. *Nature Communications* **13**: 28.

Schlesinger WH, Jasechko S. 2014. Transpiration in the global water cycle. *Agricultural and Forest Meteorology* **189–190**: 115–117.

Schuldt B, Buras A, Arend M, Vitasse Y, Beierkuhnlein C, Damm A, Gharun M, Grams TEE, Hauck M, Hajek P *et al.* 2020. A first assessment of the impact of the extreme 2018 summer drought on Central European forests. *Basic and Applied Ecology* **45**: 86–103.

Schulze E-D, Kelliher FM, Körner C, Lloyd J, Leuning R. 1994. Relationships among maximum stomatal conductance, ecosystem surface conductance, carbon assimilation rate, and plant nitrogen nutrition: a global ecology scaling exercise. *Annual Review of Ecology and Systematics* **25**: 629–662.

Sperry JS, Venturas MD, Anderegg WRL, Mencuccini M, Mackay DS, Wang Y, Love DM. 2017. Predicting stomatal responses to the environment from the optimization of photosynthetic gain and hydraulic cost. *Plant, Cell & Environment* **40**: 816–830.

Steppe K, De Pauw DJW, Lemeur R, Vanrolleghem PA. 2006. A mathematical model linking tree sap flow dynamics to daily stem diameter fluctuations and radial stem growth. *Tree Physiology* **26**: 257–273.

Steppe K, Lemeur R. 2007. Effects of ring-porous and diffuse-porous stem wood anatomy on the hydraulic parameters used in a water flow and storage model. *Tree Physiology* **27**: 43–52.

Steppe K, Sterck F, Deslauriers A. 2015. Diel growth dynamics in tree stems: linking anatomy and ecophysiology. *Trends in Plant Science* **20**: 335–343.

Trotsiuk V, Hartig F, Cailleret M, Babst F, Forrester DI, Baltensweiler A, Buchmann N, Bugmann H, Gessler A, Gharun M *et al.* 2020. Assessing the response of forest productivity to climate extremes in Switzerland using model–data fusion. *Global Change Biology* **26**: 2463–2476.

Tyree MT, Zimmermann MH. 2002. Hydraulic architecture of whole plants and plant performance. In: Tyree MT, Zimmermann MH, eds. *Xylem structure and the ascent of sap*. Berlin, Heidelberg, Germany: Springer, 175–214.

Walthert L, Ganthaler A, Mayr S, Saurer M, Waldner P, Walser M, Zweifel R, von Arx G. 2021. From the comfort zone to crown dieback: sequence of physiological stress thresholds in mature European beech trees across progressive drought. *Science of the Total Environment* **753**: 141792.

Wang Y, Sperry JS, Anderegg WRL, Venturas MD, Trugman AT. 2020. A theoretical and empirical assessment of stomatal optimization modeling. *New Phytologist* **227**: 311–325.

Wenping Y, Yi Z, Shilong P, Philippe C, Danica L, Yingping W, Youngryel R, Guixing C, Wenjie D, Zhongming H *et al.* 2019. Increased atmospheric vapor pressure deficit reduces global vegetation growth. *Science Advances* **5**: eaax1396.

Wolf A, Anderegg WRL, Pacala SW. 2016. Optimal stomatal behavior with competition for water and risk of hydraulic impairment. *Proceedings of the National Academy of Sciences, USA* **113**: E7222–E7230.

Zuur AF, Ieno EN, Elphick CS. 2010. A protocol for data exploration to avoid common statistical problems. *Methods in Ecology and Evolution* **1**: 3–14.

Zweifel R, Etzold S, Sterck F, Gessler A, Anfodillo T, Mencuccini M, von Arx G, Lazzarin M, Haeni M, Feichtinger L *et al.* 2020. Determinants of legacy effects in pine trees – implications from an irrigation-stop experiment. *New Phytologist* **227**: 1081–1096.

Zweifel R, Haeni M, Buchmann N, Eugster W. 2016. Are trees able to grow in periods of stem shrinkage? *New Phytologist* **211**: 839–849.

Zweifel R, Steppe K, Sterck FJ. 2007. Stomatal regulation by microclimate and tree water relations: interpreting ecophysiological field data with a hydraulic plant model. *Journal of Experimental Botany* **58**: 2113–2131.

Zweifel R, Sterck F, Braun S, Buchmann N, Eugster W, Gessler A, Häni M, Peters RL, Walthert L, Wilhelm M *et al.* 2021. Why trees grow at night. *New Phytologist* **231**: 2174–2185.

Zweifel R, Zimmermann L, Zeugin F, Newbery DM. 2006. Intra-annual radial growth and water relations of trees: implications towards a growth mechanism. *Journal of Experimental Botany* **57**: 1445–1459.

Supporting Information

Additional Supporting Information may be found online in the Supporting Information section at the end of the article.

Fig. S1 Relationship between predawn leaf water potential (Ψ_{leaf}) and soil water potential (Ψ_{soil}).

Fig. S2 Percentage conductance loss (PLC) curves for branches of all six species.

Fig. S3 Example of specific-specific sap flow and stem diameter dynamics.

Fig. S4 Hydraulic safety margins for all six species.

Fig. S5 Distribution of the wood anatomical variables derived from the sapwood of the six monitored species.

Fig. S6 Ring-width index sensitivity to monthly climate conditions for all six species.

Table S1 Symbol, unit and description of abbreviations used within this study.

Please note: Wiley is not responsible for the content or functionality of any Supporting Information supplied by the authors. Any queries (other than missing material) should be directed to the *New Phytologist* Central Office.